

Proton Transfer in *N*-(2-Hydroxy-1-naphthylmethylene)-1-pyrenamine and *N,N'*-Bis(2-hydroxy-1-naphthylmethylene)-*p*-phenylenediamine Crystals

Tamotsu INABE,* Isabelle LUNEAU,^{†,‡} Tadaoki MITANI,^{†,‡,##} Yusei MARUYAMA,[†] and Sadamu TAKEDA^{††}

Department of Chemistry, Faculty of Science, Hokkaido University, Sapporo 060

[†]Institute for Molecular Science, Myodaiji, Okazaki 444

^{††}Department of Chemistry, Faculty of Science, Osaka University, Toyonaka, Osaka 560

(Received August 11, 1993)

Two kinds of *N*-(2-hydroxy-1-naphthylmethylene)aniline-type compounds, *N*-(2-hydroxy-1-naphthylmethylene)-1-pyrenamine (NPY) and *N,N'*-bis(2-hydroxy-1-naphthylmethylene)-*p*-phenylenediamine (DNP), have been prepared as members of the *N*-salicylideneaniline family and subjected to structural studies in the crystalline state. In NPY, the hydrogen in the intramolecular $N\cdots H-O$ hydrogen bond has been found to locate not only at the oxygen site, but also at the nitrogen site, even at 120 K. A similar hydrogen-bond structure has also been found for DNP. This is mainly due to the π -electron delocalization effect. The relative stabilization of the proton transferred form (NH-form) compared with ordinary *N*-salicylideneanilines has been clearly indicated by solid-state NMR measurements.

N-Salicylideneaniline derivatives have been known to show a tautomerization induced by an intramolecular proton transfer from the hydroxyl oxygen to the imine nitrogen through the $O-H\cdots N$ hydrogen bond accompanying a π -electron configurational change. The tautomers produced by the proton transfer have different electronic states; sometimes this self-isomerization is observed in the crystalline state as thermochromism or photochromism.¹⁾ We are interested in these compounds, since they may be a desirable target for studying the proton–electron coupling not only in a single molecule, but also in the assembly state. Especially when the intermolecular π - π interaction is sufficiently strong, the physical properties dominated by the interaction, e.g., electrical conduction, are expected to be modulated by the proton motion or concertedly coupled with the proton motion. This coupling between protons and electrons may be utilized for designing materials which have novel types of electronic properties.²⁾

In our previous studies, several *N*-salicylideneanilines were subjected to both structural and optical analyses. With various chemical modifications, it has been found that the proton-transfer behavior, i. e., the chromatic behavior, is remarkably changed: the typical thermochromic behavior for *N,N'*-disalicylidene-*p*-phenylenediamine,³⁾ no chromatic for *N,N'*-disalicylidene-1,6-pyrenediamine,⁴⁾ and weakly thermochromic for *N*-tetrachlorosalicylideneaniline and *N*-tetrachlorosalicylidene-1-pyrenamine.⁵⁾ The variety arises from the molecular structure,⁴⁾ steric effect,⁵⁾ or intermolecular charge-transfer interaction.⁵⁾ In the present study, the aromatic ring of the aldehyde side of the Schiff base is extended; the salicylidene part is substituted by the 2-hydroxy-1-naphthylmethylene group. The effect on the proton-

transfer behavior by this substitution is described for two kinds of derivatives, NPY and DNP (Chart 1).

Experimental

Materials. NPY was prepared by the condensation of 2-hydroxy-1-naphthaldehyde and 1-pyrenylamine in refluxed methanol, and was recrystallized from benzene. Single crystals of NPY were grown by slow evaporation of the 1,2-dichloroethane solution. DNP was prepared in the same manner using *p*-phenylenediamine. Single crystals were grown by slow evaporation of the chlorobenzene solution.

Measurements. The infrared absorption spectra of single-crystal specimens were measured using a Perkin-Elmer 1650 FT-IR microscope system. For measurements of the spin-lattice relaxation rate (T_1^{-1}) of proton NMR, a pulverized specimen was dried under vacuum and sealed off into a glass ampule with helium gas of about 2 kPa. T_1^{-1} was determined by a 90° -train- τ - 90° pulse sequence. The recovery curve of the proton magnetization was expressed by a single exponential function. The temperature of the sample was measured by means of chromel-P–constantane and Au(Fe)–chromel thermocouples. The uncertainty of the temperature was between 0.1 and 0.2 K.

X-Ray Structural Analyses. Automated Rigaku AFC-5R (NPY (295 K) and DNP (295 K)) and AFC-5 (NPY (120 K)) diffractometers with graphite monochromatized Mo $K\alpha$ radiation ($\lambda=0.71073$ Å) were used for data

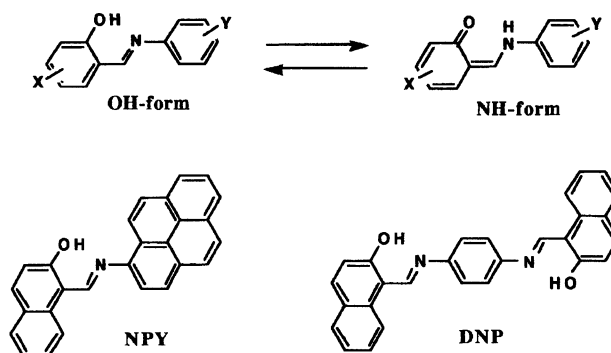


Chart 1.

*Present address: Liesg, Enseeg, Domaine Universitaire BP75, 38402 Saint-Martin D'Heres, France.

##Present address: Japan Advanced Institute of Science and Technology Hokuriku, Tatsunokuchi, Nomi, Ishikawa 923-12.

Table 1. Data-Collection Conditions and Crystal Data

	NPY		DNP
	120 K	295 K	
Range of h, k , and l	$-21 \leq h \leq 19$ $0 \leq k \leq 6$ $0 \leq l \leq 19$	$-21 \leq h \leq 19$ $0 \leq k \leq 6$ $0 \leq l \leq 19$	$-10 \leq h \leq 10$ $0 \leq k \leq 27$ $0 \leq l \leq 9$
Scan rate/ $^{\circ} \text{ min}^{-1}$	3	4	4
Number of reflections measured	3023	3055	3196
Number of independent reflections observed ($F_o > 3\sigma(F_o)$)	1586	1007	1211
Lattice parameter measurement			
2θ range/ $^{\circ}$	$22 < 2\theta < 27$	$21 < 2\theta < 29$	$22 < 2\theta < 28$
Number of reflections	24	25	25
Chemical formula	$\text{C}_{27}\text{H}_{17}\text{NO}$	$\text{C}_{27}\text{H}_{17}\text{NO}$	$\text{C}_{28}\text{H}_{20}\text{N}_2\text{O}_2$
Molecular weight	371.4	371.4	416.5
Crystal color	Brown red	Brown red	Red
Crystal size/mm	$0.55 \times 0.20 \times 0.08$	$0.55 \times 0.20 \times 0.08$	$0.23 \times 0.23 \times 0.10$
Space group	Pa	Pa	$P2_1/c$
$a/\text{\AA}$	15.277(4)	15.413(5)	7.563(2)
$b/\text{\AA}$	4.767(1)	4.815(1)	19.301(4)
$c/\text{\AA}$	13.568(4)	13.507(5)	7.102(1)
$\beta/^{\circ}$	115.06(2)	114.99(2)	106.65(2)
$V/\text{\AA}^3$	895.1(4)	908.5(5)	993.2(4)
Z	2	2	2
$D_c/\text{g cm}^{-3}$	1.378	1.358	1.393
$\mu(\text{Mo K}\alpha)/\text{cm}^{-1}$	0.78	0.77	0.82
R	0.048	0.043	0.060
R_w	0.050	0.043	0.052
Weighting factor(g) $w^{-1} = \sigma^2 + (gF)^2$	0.015	0.015	0.015

collection. The data-collection conditions are summarized in Table 1. In all cases, the intensity data were collected over the range $2\theta < 60^{\circ}$ in the θ - 2θ mode with a scan width of $(1.2 + 0.5 \tan \theta)^{\circ}$; three standard reflections monitored every 100 data measurements showed no significant deviation in intensities; the deviations were within 1.6%.

The crystal structures were solved by a direct method,⁷⁾ and the positions of all the hydrogen atoms were determined from difference synthesis maps. A block-diagonal least-squares technique (UNICS III⁸⁾) with anisotropic thermal parameters for non-hydrogen atoms and isotropic for hydrogen atoms was employed for the structure refinement.

Results and Discussion

Molecular and Crystal Structures of NPY.

The atomic parameters obtained by analyses of the X-ray diffraction at 120 and 295 K are listed in Tables 2 and 3, respectively.⁹⁾ The molecular structure at 120 K is shown in Fig. 1; the bond lengths are listed in Table 4. The molecule is nearly planar; the dihedral angle between the naphthalene and pyrene rings is 5.9° at 295 K, and does not change significantly upon cooling down to 120 K (5.6°).

The crystal structure at 120 K is shown in Fig. 2. Nearly planar molecules are stacked with each other, constructing one-dimensional columns along the b -axis. The molecular packing mode is similar to typical thermochromic *N*-salicylideneanilines. There is no remark-

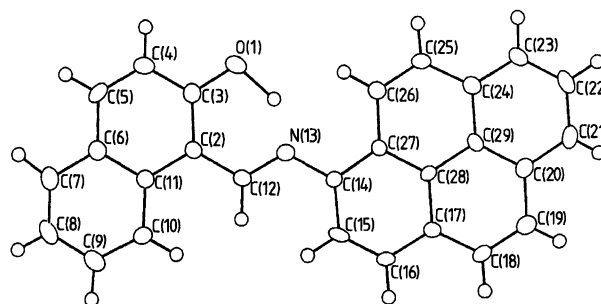


Fig. 1. ORTEP drawing of NPY at 120 K showing the atom numbering scheme.

able short contacts between the columns. Figure 3 shows the temperature dependence of the lattice parameters. They are monotonically changed upon cooling. The a - and b -axes are preferentially decreased, leading to a shortening of the distance between the mean molecular planes within the column from 3.44 Å at 295 K to 3.39 Å at 120 K. This interplanar distance is comparable to other thermochromic *N*-salicylideneanilines. The short interatomic distances within the column are shown in Fig. 4.

The most interesting point concerning this compound is the hydrogen-bond structure. It is noticeable that the CO distance in this compound at 295 K is appreciably

Table 2. Fractional Coordinates ($\times 10^4$) and Equivalent Temperature Factors for NPY at 120 K

Atom	<i>x</i>	<i>y</i>	<i>z</i>	$B_{eq}/\text{\AA}^2$ ^{a)}
O(1)	5871(2)	10968(7)	10126(2)	3.0(1)
C(2)	5003(2)	11814(8)	11212(3)	1.4(1)
C(3)	5780(3)	12357(8)	10933(3)	2.1(2)
C(4)	6494(3)	14374(10)	11519(3)	2.5(2)
C(5)	6436(3)	15851(8)	12354(3)	2.2(1)
C(6)	5666(3)	15376(8)	12672(3)	1.7(1)
C(7)	5624(3)	16896(3)	12549(3)	2.2(1)
C(8)	4897(3)	16447(9)	13866(3)	2.4(2)
C(9)	4172(3)	14506(10)	13302(3)	2.5(2)
C(10)	4183(3)	12992(8)	12436(3)	2.0(1)
C(11)	4944(3)	13357(8)	12091(3)	1.5(1)
C(12)	4287(3)	9749(8)	10625(3)	1.7(1)
N(13)	4326(2)	8321(7)	9822(3)	1.8(1)
C(14)	3628(2)	6282(8)	9230(3)	1.5(1)
C(15)	2881(3)	5427(9)	9522(3)	2.2(2)
C(16)	2223(3)	3404(8)	8940(3)	1.7(1)
C(17)	2266(2)	2098(8)	8031(3)	1.5(1)
C(18)	1593(3)	-7(8)	7411(3)	1.8(1)
C(19)	1647(3)	-1229(8)	6541(3)	2.0(1)
C(20)	2390(3)	-449(8)	6194(3)	1.6(1)
C(21)	2448(3)	-1675(8)	5289(3)	2.1(2)
C(22)	3166(3)	-868(9)	4981(3)	2.2(2)
C(23)	3844(3)	1150(9)	5566(3)	1.9(1)
C(24)	3814(3)	2426(8)	6477(3)	1.5(1)
C(25)	4495(3)	4547(8)	7107(3)	1.8(1)
C(26)	4445(3)	5784(8)	7991(3)	1.8(1)
C(27)	3709(3)	5008(8)	8336(3)	1.3(1)
C(28)	3021(3)	2900(8)	7723(3)	1.4(1)
C(29)	3067(3)	1628(8)	6794(3)	1.4(1)

a) $B_{eq} = 4/3 \sum_i \sum_j \beta_{ij} a_i a_j$.Table 3. Fractional Coordinates ($\times 10^4$) and Equivalent Temperature Factors for NPY at 295 K.

Atom	<i>x</i>	<i>y</i>	<i>z</i>	$B_{eq}/\text{\AA}^2$ ^{a)}
O(1)	5856(3)	10822(8)	10129(3)	6.7(2)
C(2)	5003(3)	11712(10)	11217(3)	3.5(2)
C(3)	5775(3)	12215(11)	10927(4)	5.0(2)
C(4)	6478(4)	14160(12)	11521(5)	5.9(3)
C(5)	6446(4)	15646(11)	12352(5)	5.8(2)
C(6)	5675(3)	15222(10)	12666(4)	4.0(2)
C(7)	5632(4)	16767(12)	13539(4)	5.4(3)
C(8)	4901(4)	16390(12)	13832(5)	6.2(3)
C(9)	4198(4)	14535(13)	13289(5)	6.4(3)
C(10)	4192(3)	12967(11)	12419(4)	4.7(2)
C(11)	4947(3)	13294(10)	12084(3)	3.9(2)
C(12)	4293(3)	9726(10)	10623(4)	4.0(2)
N(13)	4325(3)	8282(8)	9812(3)	4.1(2)
C(14)	3630(3)	6269(10)	9235(3)	3.9(2)
C(15)	2873(3)	5492(12)	9503(4)	4.7(2)
C(16)	2229(3)	3476(11)	8931(4)	4.4(2)
C(17)	2266(3)	2204(10)	8029(4)	3.7(2)
C(18)	1593(3)	128(10)	7416(4)	4.6(2)
C(19)	1653(3)	-1083(10)	6551(4)	4.7(2)
C(20)	2401(3)	-357(10)	6210(4)	4.2(2)
C(21)	2447(3)	-1591(10)	5300(4)	4.9(2)
C(22)	3169(4)	-775(12)	4990(4)	5.5(2)
C(23)	3840(3)	1149(11)	5582(4)	4.5(2)
C(24)	3807(3)	2411(10)	6486(4)	3.9(2)
C(25)	4486(3)	4459(10)	7125(4)	4.4(2)
C(26)	4441(3)	5749(10)	7992(4)	4.1(2)
C(27)	3699(3)	5017(10)	8344(3)	3.2(2)
C(28)	3018(3)	2946(9)	7728(4)	3.5(2)
C(29)	3068(3)	1677(9)	6800(3)	3.3(2)

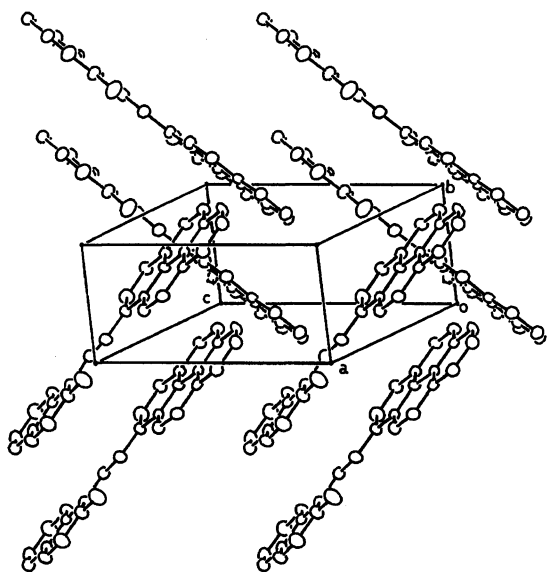
a) $B_{eq} = 4/3 \sum_i \sum_j \beta_{ij} a_i a_j$.

Fig. 2. Crystal structure of NPY at 120 K.

short (1.319(7) Å) compared with that of other typical thermochromic *N*-salicylideneanilines (1.34–1.35 Å), and is comparable to those in *N*-tetrachrolosalicylideneanilines, in which the hydrogen atom is located at

the middle of the NHO hydrogen bond. The CO bond is a single bond in the OH form and is alternated with a double bond upon tautomerization to the NH-form. Therefore, this bond length can be regarded as being an index to know how much the NH-form is populated in the crystal. Although the positions of hydrogen determined by X-ray analysis are, in general, thought to be not as precise as the CO distance, the electron density map of the hydrogen bond is useful for discussing the hydrogen-bond structure. The map is obtained by calculating the difference Fourier syntheses while taking the parameters of the hydroxyl hydrogen out of the refined structure (Fig. 5). Although the electron density in the hydrogen bond is quite featureless at 295 K, two clear peaks appear in the electron density map upon cooling down to 120 K; one corresponds to the OH hydrogen and the other to the NH hydrogen.

Molecular and Crystal Structures of DNP.

The atomic parameters of DNP obtained by an X-ray analysis at 295 K are listed in Table 5.⁹⁾ The molecular structure along with the interatomic distances is shown in Fig. 6. The dihedral angle between the central benzene ring and the terminal naphthalene rings is 21.8°. This angle is larger than that of NPY, but is

Table 4. Bond Lengths for NPY

	$l/\text{\AA}$			$l/\text{\AA}$	
	120 K	295 K		120 K	295 K
O(1)–C(3)	1.336(6)	1.319(7)	C(16)–C(17)	1.408(6)	1.387(8)
C(2)–C(3)	1.414(6)	1.422(8)	C(17)–C(18)	1.428(5)	1.427(6)
C(2)–C(11)	1.436(6)	1.430(7)	C(17)–C(28)	1.435(6)	1.426(8)
C(2)–C(12)	1.436(5)	1.420(6)	C(18)–C(19)	1.351(7)	1.344(9)
C(3)–C(4)	1.419(5)	1.401(7)	C(19)–C(20)	1.449(7)	1.458(8)
C(4)–C(5)	1.367(7)	1.349(9)	C(20)–C(21)	1.396(6)	1.395(8)
C(5)–C(6)	1.431(7)	1.434(9)	C(20)–C(29)	1.414(5)	1.400(6)
C(6)–C(7)	1.418(6)	1.420(8)	C(21)–C(22)	1.384(7)	1.400(9)
C(6)–C(11)	1.424(5)	1.412(6)	C(22)–C(23)	1.389(5)	1.367(7)
C(7)–C(8)	1.367(7)	1.355(10)	C(23)–C(24)	1.396(6)	1.383(8)
C(8)–C(9)	1.396(6)	1.356(8)	C(24)–C(25)	1.443(5)	1.431(6)
C(9)–C(10)	1.384(7)	1.393(9)	C(24)–C(29)	1.430(6)	1.417(8)
C(10)–C(11)	1.437(7)	1.424(8)	C(25)–C(26)	1.367(6)	1.354(8)
C(12)–N(13)	1.307(6)	1.315(7)	C(26)–C(27)	1.438(6)	1.454(8)
N(13)–C(14)	1.415(5)	1.410(6)	C(27)–C(28)	1.437(5)	1.433(6)
C(14)–C(15)	1.418(7)	1.410(8)	C(28)–C(29)	1.428(6)	1.425(7)
C(14)–C(27)	1.407(6)	1.390(7)	O(1)···N(13)	2.551(5)	2.530(6)
C(15)–C(16)	1.376(5)	1.370(7)			

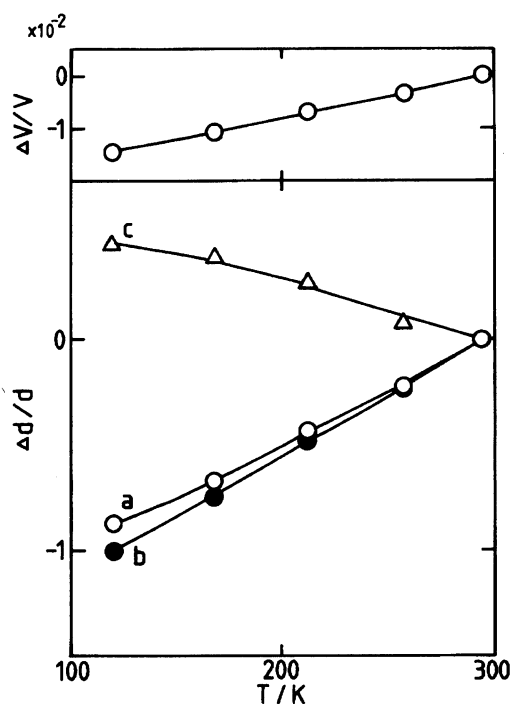


Fig. 3. Temperature dependence of the lattice parameters of NPY (d and V are the room temperature parameters and volume, respectively, $\Delta d = d(T) - d$, and $\Delta V = V(T) - V$

substantially smaller than that of N,N' -disalicylidene-1,6-pyrenediamine (42°), in which the proton transfer in the hydrogen bond is completely suppressed.⁴⁾

The crystal structure is shown in Fig. 7. In this case, the molecules related translationally along the c -axis do not directly overlap; the molecules are interleaved with another molecule related by a screw axis along the b -axis. Thus, the effective overlap is achieved only

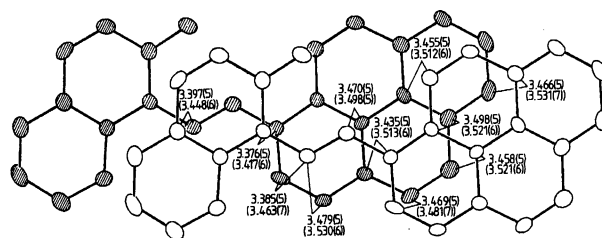


Fig. 4. Molecular overlapping between the NPY molecules and some short interatomic distances (\AA) at 120 K.

Table 5. Fractional Coordinates ($\times 10^4$) and Equivalent Temperature Factors for DNP

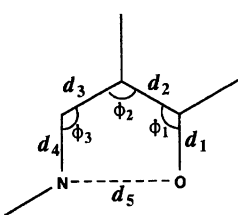
Atom	x	y	z	$B_{eq}/\text{\AA}^2$ ^{a)}
O(1)	3919(3)	1369(1)	8153(3)	4.8(1)
C(2)	6290(4)	2226(1)	8793(4)	3.1(1)
C(3)	4423(4)	2027(1)	8328(4)	3.6(1)
C(4)	3020(4)	2538(2)	8049(4)	4.1(1)
C(5)	3452(4)	3214(2)	8231(4)	4.3(1)
C(6)	5307(4)	3451(1)	8673(4)	3.7(1)
C(7)	5744(4)	4163(2)	8860(5)	4.7(1)
C(8)	7502(5)	4390(2)	9276(5)	5.1(1)
C(9)	8926(4)	3911(2)	9525(5)	4.9(1)
C(10)	8570(4)	3212(1)	9370(4)	4.0(1)
C(11)	6748(4)	2958(1)	8949(4)	3.3(1)
C(12)	7695(4)	1713(1)	9201(4)	3.6(1)
N(13)	7317(3)	1052(1)	9100(3)	3.7(1)
C(14)	8699(4)	536(1)	9536(4)	3.3(1)
C(15)	10496(4)	643(1)	9458(4)	3.8(1)
C(16)	8223(4)	-113(1)	10075(4)	3.6(1)

a) $B_{eq} = 4/3 \sum_i \sum_j \beta_{ij} a_i a_j$.

between the terminal naphthalene rings. The distances between the mean planes of the 2-hydroxy-1-naphthyl-methylene part are about 3.53 and 3.56 \AA , which are in

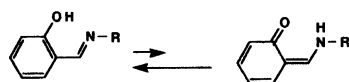
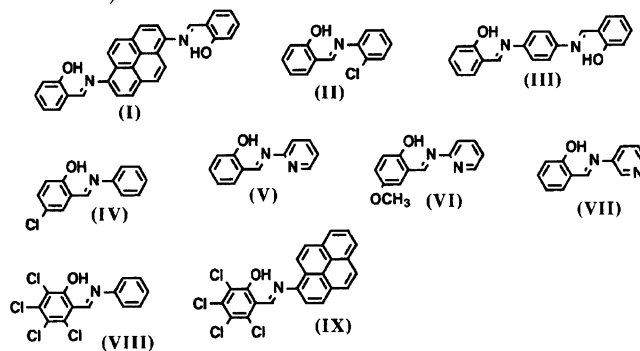
is compiled in Table 6 along with that for other *N*-salicylideneanilines. The chromatic property of these crystals spreads to a wide range from no chromatic or photochromic species, which has an asymmetric double-minimum potential of hydrogen with an extremely large energy difference and a large energy barrier compared with the thermal energy, to weakly thermochromic species, in which the potential is nearly a broad single-well or nearly a symmetric double-well with a small energy barrier. The compound(**VIII**) in Table 6 is one of the latter cases, in which a steric interaction between the Cl atom and the hydrogen at the azomethine results

Table 6. Geometry of the Hydrogen-Bonded Chelate Ring

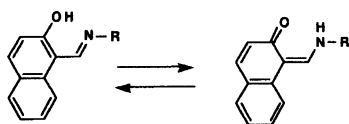


Compound ^{a)}			$d_1/\text{\AA}$	$d_2/\text{\AA}$	$d_3/\text{\AA}$	$d_4/\text{\AA}$	$d_5/\text{\AA}$	$\phi_1 + \phi_2 + \phi_3/^\circ$
(I) ^{b)}	N	(295 K)	1.356(5)	1.419(6)	1.442(6)	1.283(5)	2.614(4)	364.7
		(118 K)	1.361(4)	1.417(5)	1.452(5)	1.285(4)	2.612(3)	364.4
(II) ^{c)}	P		1.365(4)	1.391(4)	1.452(4)	1.288(4)	2.609	364.7
(III) ^{d)}	T	(295 K)	1.349(2)	1.404(3)	1.448(3)	1.284(2)	2.607(2)	365.0
		(118 K)	1.350(3)	1.406(4)	1.456(4)	1.297(3)	2.599(3)	364.2
(IV) ^{e)}	T	(R.T.)	1.351(5)	1.418(6)	1.444(6)	1.270(5)	2.584	363.7
		(90 K)	1.364(6)	1.416(7)	1.438(7)	1.292(7)	2.594	363.7
(V) ^{f)}	T		1.348(6)	1.401(6)	1.448(6)	1.285(6)		364.3
(VI) ^{f)}	T		1.343(7)	1.427(9)	1.445(8)	1.279(7)		364.9
(VII) ^{g)}	T		1.341(8)	1.409(8)	1.448(7)	1.277(9)		365.0
(VIII) ^{h)}	WT		1.332(8)	1.412(9)	1.435(9)	1.298(9)	2.512(7)	361.4
(IX) ^{h)}	WT		1.316(5)	1.423(7)	1.434(7)	1.298(6)	2.534(5)	362.8
NPY		(295 K)	1.319(7)	1.422(8)	1.420(6)	1.315(7)	2.530(6)	363.2
		(120 K)	1.336(6)	1.414(6)	1.436(5)	1.307(6)	2.551(5)	363.5
DNP			1.322(3)	1.408(4)	1.420(4)	1.305(4)	2.537(3)	363.8

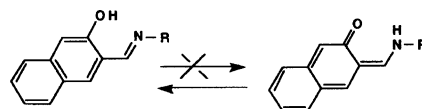
a) N; no chromatic, P; photochromic, T; thermochromic, WT; weakly thermochromic. b) Ref. 4. c) Ref. 10. d) Ref. 3. e) Ref. 11. f) Ref. 12. g) Ref. 13. h) Ref. 5.



Scheme 1.



Scheme 2.



Scheme 3.

in a contraction of the $N\cdots O$ distance. This effect also appears in the angle $(\phi_1 + \phi_2 + \phi_3)$. Comparing these values with those of NPY and DNP, it can be seen that the hydrogen-bonded chelate rings of NPY and DNP are not so much squeezed compared to compound (VIII).

Another effect which causes the hydrogen-bond structure average is an intermolecular charge-transfer inter-

action. This was found for compound (IX), in which the donor part of the molecule is overlapped with the acceptor part by stacking while alternating the molecular orientation. In this compound, there is also a steric effect similar to that of (VIII). However, as can be seen from Table 6, the degree of contraction of the hydrogen bond is not as large as that found in (VIII), and it is difficult to consider that this effect is dominant in making the CO distance even shorter than in (VIII), namely a larger population of the NH-type structure. The charge-transfer interaction operating between the molecules is considered to be the only possible explana-

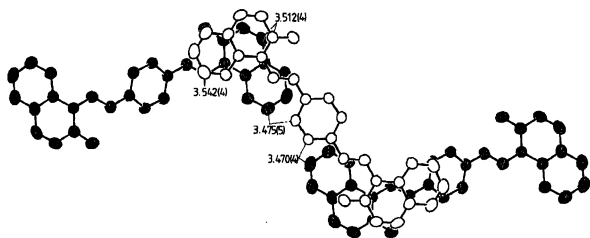


Fig. 8. Molecular overlapping between the DNP molecules and some short interatomic distances (Å).

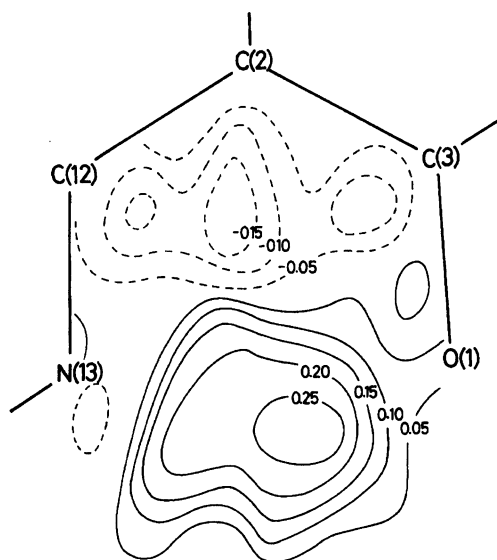


Fig. 9. Difference synthesis map of the hydrogen-bonded chelate ring (e Å^{-3}) of DNP.

tion for this modification of the hydrogen-bond structure. In the cases of NPY and DNP, it is difficult to apply the same explanation for the observed intermediate hydrogen-bond structure, since there are no such strong intermolecular charge-transfer interactions.

Here, one should note the π -electron structure in NPY and DNP. Considering the tautomerization from the OH-form to the NH-form in *N*-salicylideneaniline, the π -electron structure is considerably changed (Scheme 1).

This change from the benzenoid to the *o*-quinonoid structure is obviously accompanied by a loss of its aromaticity, leading the NH-form to an unstable state. In the case of the 2-hydroxy-1-naphthylmethylene compounds, the process of tautomerization includes a similar change only in one of the benzene ring of the naphthalene framework. The other benzene ring can keep the benzenoid structures before and after tautomerization (Scheme 2).

This is considered to be a dominant mechanism which leads to a much smaller energy difference between the OH and NH forms compared with the case of ordinary *N*-salicylideneanilines.

Infrared Spectra and Nuclear Magnetic Resonance. The OH and/or NH stretching mode in

N-salicylideneanilines has been found to be detected by using single-crystal specimens; otherwise, the broad peak is completely smeared out for powder dispersed nujol mull or KBr discs.³⁾ Figure 10 shows the IR spectra of NPY and DNP at room temperature. In the case of NPY, the molecular plane is largely deviated from a plane normal to the stacking axis, so that in-plane modes are not clearly separated from out-of-plane modes. The broad humps lying in the range from 2450 to 3550 cm^{-1} are assignable to the OH and/or NH stretching mode. Since the humps are overlapped with the CH stretching mode at 3049 cm^{-1} , the exact structure of the band, i. e., constructed by two bands or a broad single band with some fine structures, is not clear.

The planes involving the hydrogen bond in DNP are nearly parallel to a plane normal to the stacking axis. The IR spectra with different polarizations with respect to the stacking axis clearly exhibit different intensities, as shown in Fig. 10(b). The broad peak at 2670 cm^{-1} in the spectrum with polarization $\perp c$ can be assigned to the OH and/or NH stretching mode, since the peak is absent in the spectrum with polarization $\parallel c$. In the latter spectrum, the CH stretching mode is clearly observed, though it is also an in-plane mode. As can be seen from the crystal structure, the aromatic rings, particularly the central benzene ring, are tilted from a plane normal to the *c*-axis, leading to a contribution of the in-plane modes to the spectrum with polarization parallel to the *c*-axis.

Compared with the infrared spectra of other *N*-salicylideneanilines, the following points are remarkable for these *N*-(2-hydroxy-1-naphthylmethylene)aniline-type compounds. First, the intensity of the OH and/or NH stretching mode is very weak, which is clearly seen by comparing it with that of the CH stretching band. The OH and/or NH stretching band was found to be broad, but much more intense than the CH stretching in the cases of no chromatic *N,N*-disalicylidene-1,6-pyrenediamine (DSPY)⁴⁾ and typical thermochromic *N,N*-disalicylidene-*p*-phenylenediamine (BSP).³⁾ Secondly, the half width of the OH and/or NH stretching band is large, ca. 900 cm^{-1} (assuming a single broad band) for NPY and ca. 670 cm^{-1} for DNP, which are larger than that of BSP (550 cm^{-1}) and of DSPY (520 cm^{-1}),^{3,4)} and rather comparable to compounds (VIII) and (IX) in Table 6.⁵⁾ These features are consistent with the intermediate hydrogen-bond structures derived from the X-ray diffraction data.

Solid-state NMR measurements, especially the spin-lattice relaxation rate (T_1^{-1}) of the proton, are expected to be useful for obtaining detailed information concerning the proton dynamics in the hydrogen bond in the crystalline state. Precise measurements of the T_1^{-1} of the typical thermochromic crystal of BSP have already been performed at 9.2 and 37.5 MHz;⁶⁾ it has been found that the temperature dependence of T_1^{-1} , which showed two separate maxima near 70 and 170 K, can be ex-

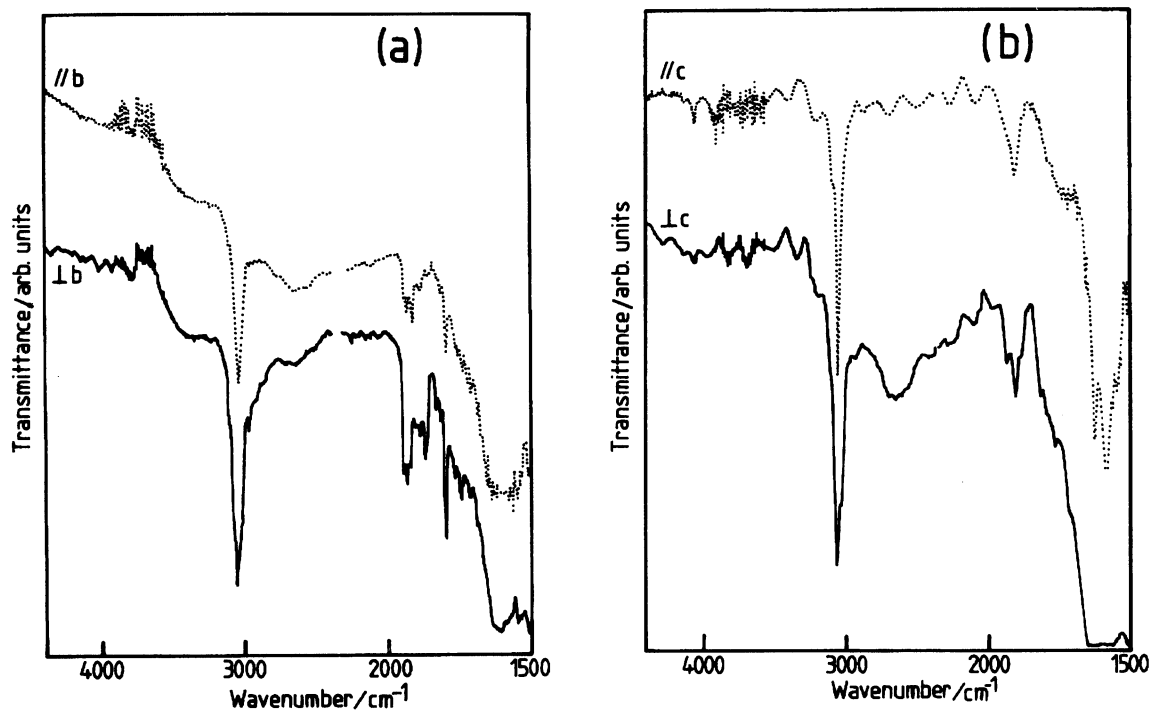


Fig. 10. Single-crystal infrared spectra of NPY (a) and DNP (b).

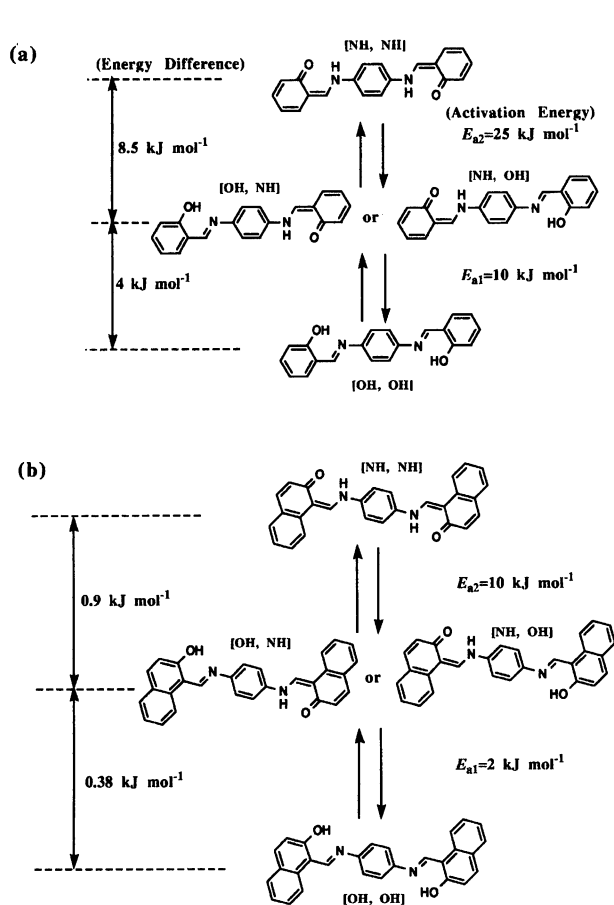


Fig. 11. Energy diagram for the proton transfer in BSP (a) and DNP (b) estimated from NMR measurements.

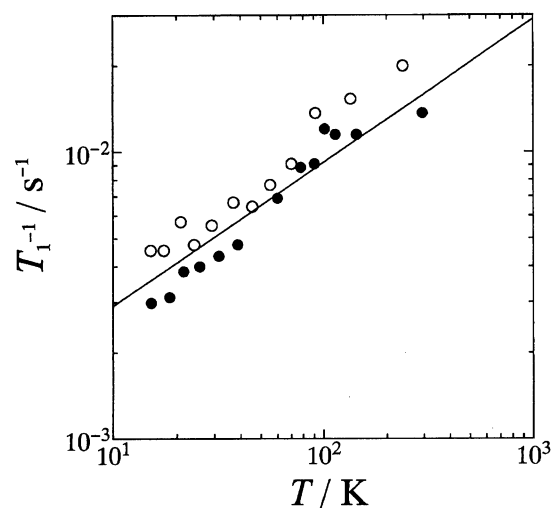


Fig. 12. The temperature dependence of the spin-lattice relaxation rate of proton of NPY (●; measured at 37 MHz and ○; measured at 18 MHz). The solid line indicates a linear correlation with square root of temperature.

plained by the same picture proposed for the mechanism of the thermochromism, namely, the proton transfer from the hydroxyl oxygen to the imine nitrogen in the hydrogen bond is accompanied by a rearrangement of the π -electron configuration. Compared with T_1^{-1} of BSP, the observed two separate T_1^{-1} maxima of DNP at 18.0 and 37.0 MHz located near to 25 and 150 K are large and the slopes of T_1^{-1} vs. the temperature are much smaller. The energy scheme between the structures obtained from the experimental results is shown

in Fig. 11. Since these molecules have two hydrogen bonds, it is considered that there are three kinds of molecular states: both OH, [OH, OH]; one half transferred, [NH, OH] or [OH, NH]; and both transferred, [NH, NH]. If the energies relevant to the first step, [OH, OH] to [OH, NH] or [NH, OH], are different from those of the second step, [OH, NH] or [NH, OH] to [NH, NH], the temperature dependence and two maxima of T_1^{-1} can be reasonably interpreted.⁶⁾ According to this model, the energy difference in BSP was estimated to be 4 kJ mol⁻¹ between [OH, OH] and [OH, NH] or [NH, OH], and 8.5 kJ mol⁻¹ between [OH, NH] or [NH, OH] and [NH, NH]. The jumping among the three energetically different states of BSP was described by classical Arrhenius processes. The jump rate from [OH, OH] to [OH, NH] or [NH, OH] was described by $4.5 \times 10^{12} \text{ (s}^{-1}\text{)} \exp(-10 \text{ (kJ mol}^{-1}\text{)}/RT)$ and the backward jump rate was $4.5 \times 10^{12} \text{ (s}^{-1}\text{)} \exp(-6 \text{ (kJ mol}^{-1}\text{)}/RT)$, while the jump rate from [OH, NH] or [NH, OH] to [NH, NH] was $4.5 \times 10^{12} \text{ (s}^{-1}\text{)} \exp(-25 \text{ (kJ mol}^{-1}\text{)}/RT)$ and the corresponding backward jump rate was $4.5 \times 10^{12} \text{ (s}^{-1}\text{)} \exp(-16.5 \text{ (kJ mol}^{-1}\text{)}/RT)$, where R is the gas constant (8.314 J K⁻¹ mol⁻¹). In DNP, the corresponding energy separations are 0.38 and 0.9 kJ mol⁻¹, respectively, as shown in Fig. 11, which are much smaller than those for BSP and correspond to a much larger population of the NH-form at room temperature than in BSP. Furthermore, an analysis of the temperature dependence of the proton-transfer rate suggests that the protons in DNP move much more easily than those in BSP by a tunneling effect.^{6,14)}

The proton dynamics in NPY has also been studied by the NMR technique. The temperature dependence of T_1^{-1} shown in Fig. 12 is not a regular type; T_1^{-1} seems to depend linearly on a square root of the temperature. The observed values of T_1^{-1} is on the order of those expected from the nuclear dipole interaction between ¹H and ¹⁴N in a hydrogen bond which is modulated by a proton transfer.

If we assume that the Arrhenius plot of T_1^{-1} is meaningful for NPY, the energies accompanied by the proton transfer may be estimated to be 0.5 kJ mol⁻¹ (40 cm⁻¹) above 60 K and 0.1 kJ mol⁻¹ (8 cm⁻¹) between 15 and 40 K from the slope of T_1^{-1} . The small energies make us imagine a tunneling of the proton in the NHO hydrogen bond with a very small energy difference (0.1 kJ mol⁻¹) between the NH- and OH-forms; however, a full profile of T_1^{-1} , including the frequency dependence, could not be explained by a model of phonon-assisted tunneling,¹⁵⁾ which is successful for the case of DNP.

The linear dependence of T_1^{-1} on \sqrt{T} may be interpreted by the collective motion of the protons within a stacking column, i. e., kink formation with regard to the position of the protons in the NHO hydrogen bonds in successively stacked NPY molecules and its diffusion along the one-dimensional stacking column axis. A kink is formed in the case in which the interaction between

the neighboring hydrogen bonds in a column is sufficiently large compared with the energy barrier for the proton transfer in a molecule. On one side of the kink, hydrogen atoms stay at the O-site in individual hydrogen bonds, while hydrogen atoms stay at the N-site on the other side of the kink. Both OH- and NH-forms thus exist in the crystal. The kink motion is accompanied by a collective transfer of protons in individual hydrogen bonds from the N- to O-site (or O- to N-site). A time correlation function for the proton motion due to the kink diffusion has been reported,¹⁶⁾ from which T_1^{-1} was calculated for the case of kink diffusion with strong friction. The derived formula of T_1^{-1} shows a linear dependence on the square root of the temperature, the behavior of which was observed for NPY, if the number of kink is effectively independent of the temperature. The frequency dependence of $T_1^{-1} \propto \omega^{3/2}$, where ω is the Larmor frequency, was predicted in the classical limit, while the observed dependence is very weak, probably due to a quantum effect. Although this hypothetical interpretation should be verified by other experiments, the results suggesting a collective motion of the proton and comparable populations of the OH- and NH-forms in time average correspond to the averaged hydrogen-bond structure evidenced by the X-ray structure analysis.

The result of an NMR measurement on DNP indicates a small energy difference between the OH- and NH-forms, and almost a comparable population of the two forms, which is consistent with hydrogen-bond structure derived from the X-ray structure analysis. Recently, a comparable population of the NH- and OH-forms in DNP at room temperature was clearly demonstrated by N and O K-XANES spectroscopy.¹⁷⁾ Therefore, so far, all of the experimental results are consistent with the hydrogen-bond structure in which the proton exists both at the oxygen site and at the nitrogen site due to the dynamic motion. From the π -electron structures of NPY and DNP, the stabilization of the NH-form is considered to result from the small energy difference between the tautomers, due to the resonance structure in the 2-hydroxy-1-naphthylmethylene derivatives. It was also noticed that Schiff bases constructed with 1-hydroxy-2-naphthaldehyde, 2-hydroxy-1-naphthaldehyde, 3-hydroxy-2-naphthaldehyde, and 2-methoxy-1-naphthaldehyde could be divided into two groups.¹⁸⁾ The compounds comprising the former two aldehydes were deeply colored at room temperature, and the color was slightly changed by temperature. On the other hand, the Schiff bases comprising the latter two aldehydes were lightly colored, and showed no response to a temperature change. These results can be interpreted as follows.

Since the proton transfer in 3-hydroxy-2-naphthylmethylene compounds is inevitably accompanied by a complete destruction of its aromaticity at the aldehyde side, the NH-form is considerably unstable compared

with the OH-form, leading to a suppression of thermochromism (Scheme 3). On the other hand, 2-hydroxy-1-naphthylmethylene or 1-hydroxy-2-naphthylmethylene compounds can undergo a proton transfer while keeping their aromaticity. Therefore, the NH-form is not so much unstable.

In conclusion, the two *N*-(2-hydroxy-1-naphthylmethylene) aniline-type compounds studied here were found to have hydrogen bonds in which the proton is located at both the oxygen and nitrogen sites. The origin of this is considered to be a resonance stabilization of the NH-form compared with salicylidene derivatives. This structural feature is well demonstrated by the frequency and band shape of the OH (and/or NH) stretching mode in the infrared spectra and in the energy separation between the OH- and NH-forms derived from the spin-lattice relaxation rate of the proton NMR.

This work was partly supported by the Asahi Glass Foundation.

References

- 1) M. D. Cohen, G. M. J. Schmidt, and S. Flavian, *J. Chem. Soc.*, **1964**, 2041.
- 2) T. Inabe, *New J. Chem.*, **15**, 129 (1991); T. Mitani, *Mol. Cryst. Liq. Cryst.*, **171**, 343 (1989).
- 3) N. Hoshino, T. Inabe, T. Mitani, and Y. Maruyama, *Bull. Chem. Soc. Jpn.*, **61**, 4207 (1988).
- 4) T. Inabe, N. Hoshino, T. Mitano, and Y. Maruyama, *Bull. Chem. Soc. Jpn.*, **62**, 2245 (1989).
- 5) T. Inabe, I. Gautier-Luneau, N. Hoshino, K. Okaniwa, H. Okamoto, T. Mitani, U. Nagashima, and Y. Maruyama, *Bull. Chem. Soc. Jpn.*, **64**, 801 (1991).
- 6) S. Takeda, J. Chihara, T. Inabe, T. Mitani, and Y. Maruyama, *Chem. Phys. Lett.*, **189**, 13 (1992).
- 7) P. Main, L. Lessinger, M. M. Woolfson, G. Germain, and J. -P. Declercq, "MULTAN78," Univ. of York, England and Louvain, Belgium (1978).
- 8) T. Sakurai and K. Kobayashi, *Rep. Inst. Phys. Chem. Res.*, **55**, 69 (1979).
- 9) The lists of structure factors, anisotropic thermal parameters for non-hydrogen atoms and parameters for hydrogen atoms are deposited as Document No. 67013 at the Office of the Editor of Bull. Chem. Soc. Jpn.
- 10) J. Bregman, L. Leiserowitz, and K. Osaki, *J. Chem. Soc.*, **1964**, 2086.
- 11) J. Bregman, L. Leiserowitz, and G. M. Schmidt, *J. Chem. Soc.*, **1964**, 2068.
- 12) I. Moustakali-Mavridis and E. Hadjoudis, *Acta Crystallogr., Sect. B*, **34**, 3709 (1978).
- 13) I. Moustakali-Mavridis, E. Hadjoudis, and A. Mavridis, *Acta Crystallogr., Sect. B*, **36**, 1126 (1980).
- 14) S. Takeda, manuscript in preparation.
- 15) J. L. Skinner and H. P. Trommsdorf, *J. Chem. Phys.*, **89**, 897 (1988).
- 16) J. L. Skinner and P. G. Wolynes, *J. Chem. Phys.*, **73**, 4015 (1980).
- 17) K. Oichi, E. Ito, K. Seki, T. Araki, S. Narioka, H. Ishii, T. Okajima, T. Yokoyama, T. Ohta, T. Inabe, and Y. Maruyama, *Jpn. J. Appl. Phys.*, **32**, Suppl. 32-2, 818 (1993).
- 18) M. D. Cohen, Y. H. Hirshberg, and G. M. J. Schmidt, *J. Chem. Soc.*, **1964**, 2060.